

# Assessment, validation, and visualisation of bony changes in crano-facial surgery

Gert Wollny and Frithjof Kruggel  
Max-Plank-Institute of  
Human Cognitive and Brain Sciences  
Stephanstr 1a  
04103 Leipzig, Germany  
{wollny,kruggel}@cbs.mpg.de

Thomas Hierl and Jörg Hendriks  
Department of Oral and  
Maxillo facial Plastic Surgery  
University of Leipzig  
Nürnberger Str. 57  
04103 Leipzig, Germany  
Thomas.Hierl@medizin.uni-leipzig.de

## ABSTRACT

Mid-facial distraction osteogenesis is a novel promising method to correct severe mid-facial hypoplasia and retrognathia. Although aesthetic improvements are obvious, the analysis of three-dimensional bony changes created through distraction was impossible so far. Now, we present a tool chain employing voxel based registration and 3D visualisation to assess and analyse the structural changes induced by the treatment based on the routinely acquired pre- and post-operative CT images. A landmark based validation of the voxel-based registration provides measures to rate the obtained results. Application to real patient data demonstrates that this tool chain can help to get a better perception of the complex three dimensional deformations of the skull during treatment.

## KEY WORDS

Image Processing and Analysis, Medical Imaging, Registration, Visualisation

## 1 Introduction

Severe malformations of the mid-face such as maxillary retrognathia or hypoplasia can be treated by distraction osteogenesis [1, 2, 3]. During an operation the appropriated bony part of the mid-face is separated from the rest of the skull (osteotomy) and later the mid-face is slowly advanced by a halo-borne distraction device (RED system) until correction of mid-facial deficiency is achieved (Fig. 1). In complex malformations operation planning is based on CT images, followed by a modified mid-facial osteotomy. Finally, the mid-face is slowly advanced by a halo-borne distraction device (RED system, Fig. 1) until correction of mid-facial deficiency is achieved.

Although striking aesthetic improvements are obvious (Fig. 1), by now, no studies regarding the analysis of the complex three-dimensional mid-facial movements are available. Incorrect treatment planning, however, leads to a malpositioned mid-face [4] and necessitates further surgical intervention. This is especially crucial, as large distances are usually treated in distraction osteogenesis and

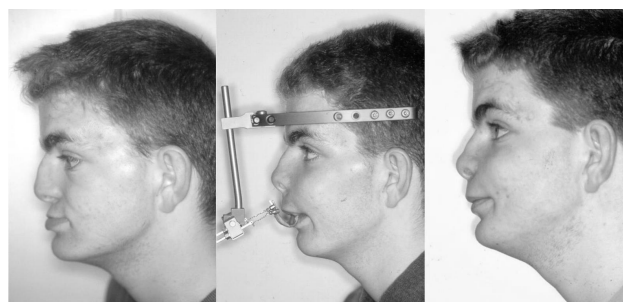


Figure 1. An 18-year-old boy with an isolated non-syndromic mid-facial hypoplasia (left). Distraction with a halo-borne external distraction device after an almost complete osteotomy (middle) led to a harmonic maxillo-mandibular relationship and improved esthetics (right).

thus small angular deviations can cause clinical failure. Only basic studies on primates have been carried out 20 years ago by Nanda et al. [5, 6] that investigated the relation of point of force application and mid-facial rotational moments. They assumed that the centre of resistance of the maxilla can be found above the root apex of the premolars and that applying a force caudal of this point results in an anterior rotation of the maxilla leading to resp. increasing an anterior open bite. However, a thorough analysis of these mid-facial movements is still pending. Yet, such analysis is necessary to get a better understanding of the effects of the distractor onto the whole skull, and thus, to improve therapy planning.

The contribution of this paper is the development and application of a tool chain that helps to give an insight into several clinically important issues: first, how do different parts of the mid-face react to a certain force applied via distraction osteogenesis. Here the point of force application and the direction of force, which can be calculated from lateral cephalograms with the mounted distractor have to be considered. Secondly, is there a centre of rotation which can be influenced by proper treatment planning? Here the clinical importance is to avoid an unwanted counter-clockwise mid-facial rotation which would lead to

an "open" bite demanding further surgery. The last issue is the new technique of sutural distraction, where no or only limited osteotomies are performed [7]. Here no information on the impact on different anatomic regions is known so far.

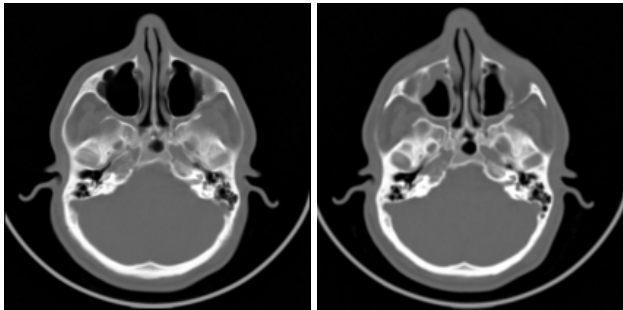


Figure 2. Example slices of pre- (left) and postoperative acquired CT scans of a patient treated by mid-facial distraction osteogenesis.

In the following, we will present the tools to assess and visualise the structural changes induced by the treatment, based on the routinely acquired pre- and post-operative *Computer topographic* (CT) images (Fig. 2). With the application to patient data, we will show that this tool chain can help to get a better perception of the complex three dimensional deformations of the skull during treatment and we discuss the validation of the obtained results.

## 2 Description of tools

In order to assess and visualise the bony changes induced by the distraction osteogenesis the following steps are required:

- *rigid registration* to correct the input images for differences in position and orientation,
- *non-rigid registration* to quantify the differences between the pre- and postoperative images describing the structural change,
- *landmark picking* for validation purposes, and
- *visualisation* to explore the changes.

In the following these steps will be outlined in more detail.

### 2.1 Registration

Registration aims at transforming a study image  $S$  with respect to a reference image  $R$  by means of a transformation  $T \in \Theta$  ( $\Theta$  is the set of possible transformations), so that structures at the same coordinates in both images finally represent the same object. In practice, this is achieved by

finding a transformation  $T_{\text{reg}}$  which minimises a cost function  $F_{\text{cost}}$ , while constraining the transformation through the joint minimisation of an energy term  $E(T)$ :

$$T_{\text{reg}} := \arg \min_{T \in \Theta} (F_{\text{cost}}(S_T, R) + \kappa E(T)). \quad (1)$$

The cost function  $F_{\text{cost}}$  accounts for the mapping of similar structures.  $E(T)$  ensures topology preservation, which is necessary to maintain structural integrity in the study image, and it thus introduces a smoothness constraint on the transformation  $T_{\text{reg}}$ . The parameter  $\kappa$  is a weighting factor that balances registration accuracy and transformation smoothness.

By restricting the set of possible transformation  $\Theta$  to rigid transformations, i.e. to *rotation* and *translation*, topology is preserved *per se*, we may set  $\kappa = 0$  and *rigid registration* is obtained by minimising the cost function  $F_{\text{cost}}$ . CT images are normalised by the *Hounsfield scale* [8], mapping similar materials to similar intensities. Therefore, we obtain rigid registration by minimising the *Sum of Squared Differences* (SSD)

$$F_{\text{cost}}(S, R) := \int_{\Omega} (S(\vec{x}) - R(\vec{x}))^2 d\vec{x}. \quad (2)$$

using a modified *Marquardt-Levenberg* algorithm [9].

If  $\Theta$  is not restricted, we require  $\kappa > 0$  and we target for *non-rigid registration*.

Two groups of methods to achieve registration may be considered: Feature-based approaches use information from identifiable brain structures, such as landmarks, curves, and surfaces. These structures have to be extracted and set into correspondence. The distance between corresponding features yield a cost function  $F_{\text{cost}}$  that has to be minimised. The spatial transformations, resulting from feature matching, are finally propagated to the whole volume by using some energy constraint  $E(T)$ , e.g., thin-plate splines [10]. Landmarks provide an effective constraint for registration, but acquiring the required dense set of corresponding Landmarks is a difficult and time consuming task [11] and it might even be impossible.

In voxel based approaches, on the other hand, the cost function  $F_{\text{cost}}$  is derived from local or global image intensity similarity measures. The advantage of these methods lies in the independence of human interaction which makes voxel based approaches the tool of choice when it comes to the automatic analysis of large sets of data. Like proposed by Christensen [12], we employ *fluid dynamics* as energy constraint  $E(T)$  - since it allows for large deformations - and we minimise SSD (2).

However, especially in the case of large differences between the images, the mapping of structures resulting from non-rigid registration might be simply wrong, i.e. corresponding identifiable structures, as used in feature based approaches, may not map onto each other. Therefore, the application of voxel-based non-rigid registration to analyse image data requires a validation of the results [13], in order

to give error margins for the findings described by the transformation  $T_{\text{reg}}$ . Thus, we turn our focus to the acquisition of a sparse set of landmarks that can be used for validation.

## 2.2 Volume rendering for manual landmark picking

In CT images, bone is mapped to high intensities and soft tissue is mapped to low intensities [8]. Therefore, volume rendering the CT image by using an appropriate intensity threshold (or *iso value*) can be employed to visualise the iso-surfaces corresponding to skin and/or bone. Consequently, we implemented a 3D texture based volume renderer that allows an intuitive interactive specification of the iso-value, in order to pick landmarks on bone and skin. Here, the volume data set is stored into a 3D RGBA texture - the alpha component is fed with the image intensity, and for shading the range compressed and normalised image gradient is stored into the RGB channels. An iso-surface can then be viewed by selecting an appropriate alpha threshold (see 3) and diffuse lighting is evaluated based on the image gradient and the global light direction (cf. e.g. [14]). With the recent advances in the graphics hardware, it is possible to implement this iso-surface browser on low cost hardware and still obtain frame rates above 20 fps.

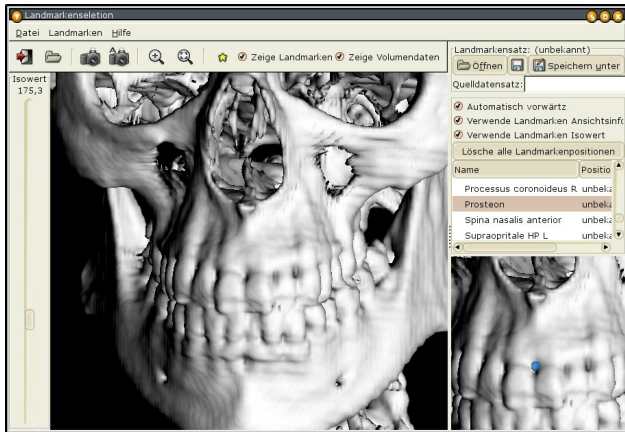


Figure 3. By selecting a landmark from the list, the main view is adjusted to a pre-defined optimal viewing direction, an appropriate iso-value is set and an image, identifying the landmark in a template image is displayed below the landmark list. Hence, the landmark can easily be selected, even without expert knowledge.

In order to support landmark picking without medical expert knowledge, a template landmark list with 33 easily identifiable landmarks was created (cp. Table 1). Besides the landmark name and its location, for each landmark an optimal view-port configuration and an iso-value are stored as well as an image that displays the landmark location in an example data set. With this support it is possible even for non-experts to pick all pre-defined anatomical landmarks

with high certainty (see Fig. 3).

## 2.3 Result visualisation

To visualise the shape change of the skull, knowledge about its geometry is necessary. Therefore, surface based rendering will be used, and hence, the skull surface has to be extracted from the segmented (and rigidly registered) data sets by using, e.g., the *marching tetrahedra* algorithm [15]. Then, the skull surface is represented by a triangle mesh which is described by a set of vertices and the corresponding (triangle-) connectivity. In order to improve the response times of the interactive visualisation, this mesh is then optimised to reduce its triangle count, without losing geometric detail [16, 17]. Finally, the shape change described by the non-rigid transformation  $T$  is visualised in the following manner: At each vertex  $\vec{x}$  of the triangle mesh the corresponding deformation vector is displayed as an arrow. Since we track the voxels from their final position on, the arrow ends at the skull surface (Fig. 4).

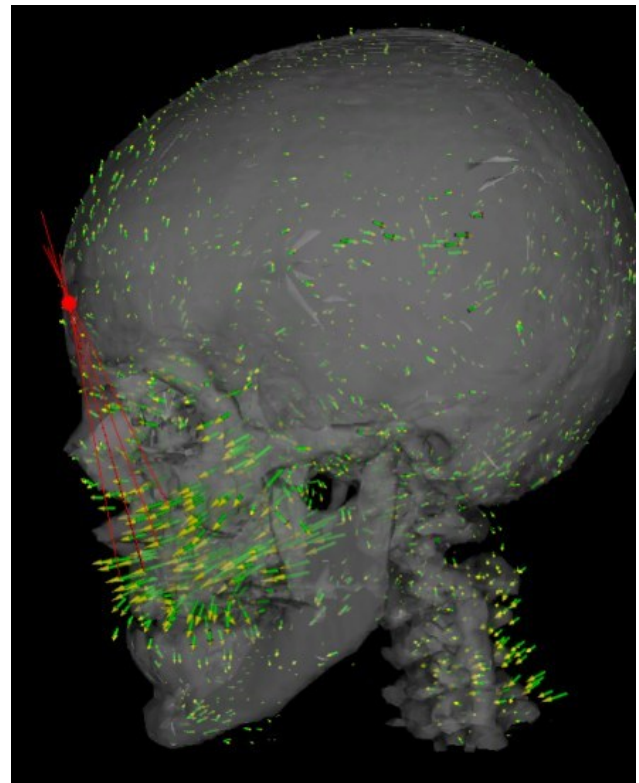


Figure 4. Shape changes of the skull induced by sutural mid-facial distraction osteogenesis (first patient). The red dot indicates the manually extracted centre of rotation.

Alternatively, the shape change of the skull is illustrated by a colouring scheme. For each vertex of the surface, the displacement vector is decomposed into its normal and tangential components. Inward-pointing normals are coded in red, outward-pointing in blue; colour intensity reflects its magnitude, the colour scale is given in mm

(Fig. 5). The colour values obtained at each vertex are propagated to the corresponding triangle by using ground shading.

### 3 Results and discussion

The data of 20 patients treated by mid-facial distraction osteogenesis were analysed employing the described tool chain.

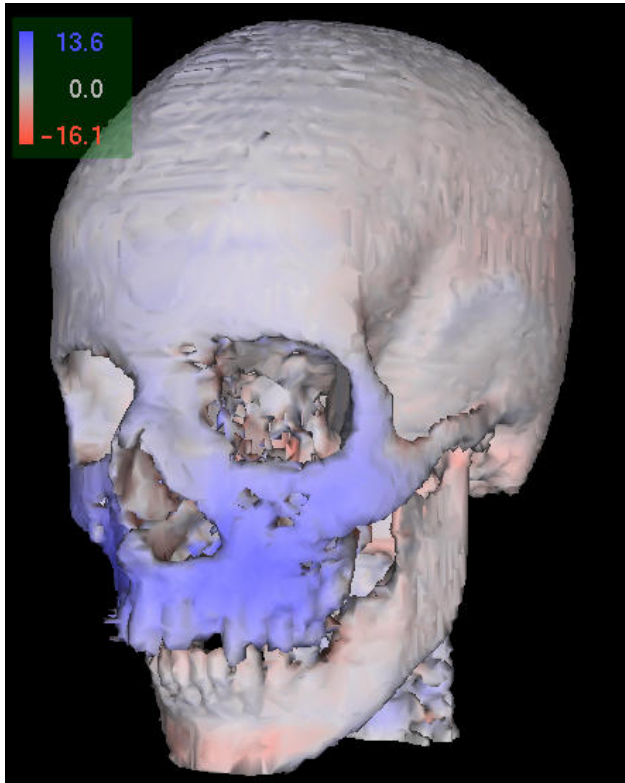


Figure 5. Shape changes of the skull induced by sutural mid-facial distraction osteogenesis (first patient). Note the blue colouring of the zygomatic bones indicating the reaction of the adjacent sutures.

A first patient, a 12-year-old boy, was suffering from a severe mid-facial hypoplasia, resulting from bilateral cleft lip and palate. He was treated by way of sutural mid-facial distraction osteogenesis with simultaneous transversal maxillary expansion, by applying the RED system for 10 weeks. The treatment resulted in a 17 mm forward displacement of the mid-face with an (intended) back slide of 2 mm later on. The retrospectively performed analysis indicated that the distraction triggered a forward shift of the zygomatic and nasal bones since the maxilla was not mobilised intra-operatively. Thus the whole mid-face showed a complex advancement caused by distraction (Fig. 5). Furthermore, the centre of rotation which is dependent on the centre of resistance and the point of applied force could be determined manually (Fig. 4); its location is important

in treatment planning and outcome, and was selected properly in this case.

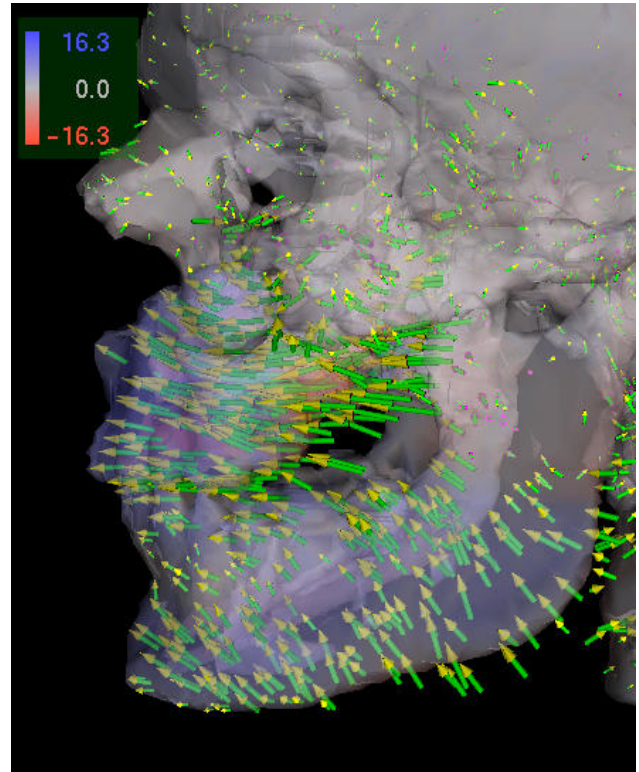


Figure 6. A close inspection of the mid-facial area emphasises, that only a forward shift of the mid-face occurred.

The second patient was an 18-year-old boy with isolated non-syndromic mid-facial hypoplasia. Distraction after an almost complete osteotomy led to a harmonic maxillo-mandibular relationship and improved aesthetics. Utilising the visualisation tools showed the complex inter-related changes caused by the forward displacement. Looking at the vectors, a straight anterior movement parallel to the occlusal plane (which was planned in before) is evident (Fig. 6). In contrast to the above case, as a result of the almost complete osteotomy the zygomatic bones were not influenced in this case (Fig. 7).

The landmark based validation showed, that in most cases the applied non-linear registration yields acceptable results. In average the registration error at the selected landmarks was below 4mm (Table 1). This error margin corresponds to errors that may be introduced because of the the image resolution of  $1mm^3$  and the landmark pick error of  $\approx 1mm$  per data set.

However, in some cases the disease pattern (e.g. cleft lip and palate) makes the identification of important landmarks of the mid-facial area (like, e.g., the *prosthion* or the *spina nasalis anterior*) and, hence, the landmarks based validation of the non-linear registration, difficult or even impossible. Additionally, it has to be noted that in some

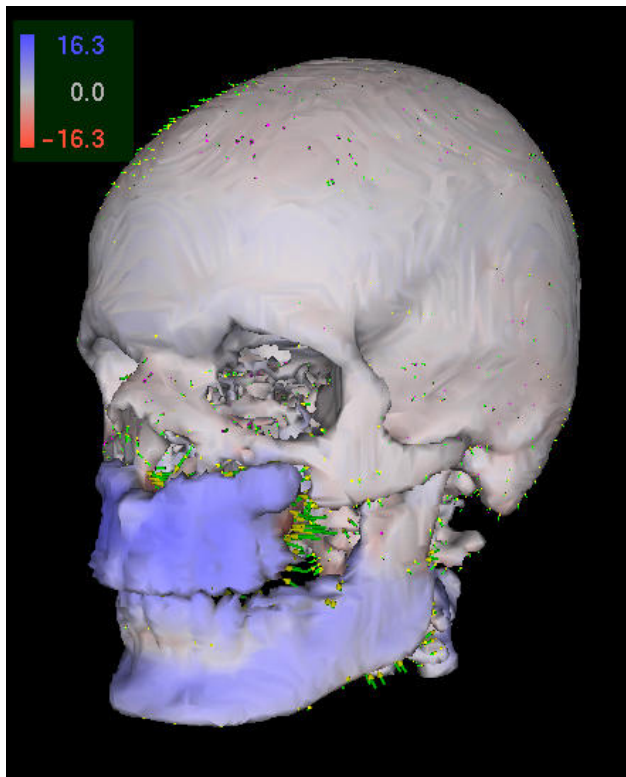


Figure 7. Shape change of the skull induced by mid-facial distraction osteogenesis (second patient). Note, that in this case the zygomatic bones were not influenced by the distraction, because of an almost complete osteotomy of the maxilla.

cases the non-linear registration partially fails, resulting in errors above 5mm. Therefore, the analysis tool chain is well suited to obtain an over-all impression of the bony changes, but a quantitative analysis can only be obtained in “well posed” cases.

## Conclusions

We proposed and applied a tool chain combining methods of image registration and visualisation to solve an important clinical problem related to mid-facial distraction osteogenesis. Our results demonstrated that the assumptions of Nanda et al. [5, 6] regarding the relation of point of force application and the mid-facial rotation are valid in mid-facial distraction. In the cases shown in this paper, a high point of force application above the maxillary plane via a bone-anchored mini-plate system leads to no or only minor counter-clockwise rotation. This implies, that this anatomical level is superior to an inferior point of force application via a dental splint used in all other studies where usually some open bite is seen postoperatively [18]. Regarding sutural distraction our tool chain helped to analyse complex bony changes which affected maxilla, zygoma, nasal bones and even the anterior cranial base.

Landmark name	average error in mm
Bregma	3.5
Earlobe (l)	2.3
Earlobe (r)	1.6
Foramen mentale L	2.0
Foramen mentale (r)	1.6
Fronto-zygomatic suture (l)	1.2
Fronto-zygomatic suture (r)	1.2
Glabella	2.5
Gnathion	3.3
Gonion (l)	1.9
Gonion (r)	2.5
Infraorbitale (most caudal point) (l)	1.6
Infraorbitale (most caudal point) (r)	1.8
Lambda	3.3
Lateral kanthus (l)	2.2
Lateral kanthus (r)	2.8
Medial kanthus (l)	1.7
Medial kanthus (r)	1.6
Nasion (bone)	2.1
Nasion (skin)	1.8
Nose tip	1.6
Opisthion	0.7
Piriform aperture (r)	2.5
Piriform aperture (l)	2.7
Processus coronoideus (l)	0.9
Processus coronoideus (r)	1.1
Prosthion	2.9
Rhinion	1.8
Spina nasalis anterior	2.7
Supraorbitale (most cranial point) (r)	2.2
Supraorbitale (most cranial point) (l)	1.8
Tuberculum mentale (l)	3.9
Tuberculum mentale (r)	3.3

Table 1. Landmarks considered for validation and average registration error in mm.

The experimental results of Nanda seen in primates compared favourably to human findings. In the first patient an anatomically high point of force application via a bone anchored retention system was correlated with almost no counter-clockwise rotation. In conclusion it can be stated that our tools provided the means to explain the bio-mechanical reasons why the treatment worked well in all patients. This is important in the understanding of how mid-facial distraction osteogenesis works and helps in future therapy planning.

Limitations of the analysis method can be found in the limitation of voxel based non-linear registration that the mapping of corresponding structures sometimes simply fails. We hope to improve the registration results by adding sparse landmark information to the registration criterion. Additionally, we will consider an automatic registration quality assessment, in order to measure the applica-

bility of the registration result for a quantitative analysis.

## Acknowledgements

Our work is supported by the European Commission under grant IST-2001-37153 (GEMSS Project).

## References

- [1] J. W. Polley and A. A. Figueroa. Management of severe maxillary deficiency in childhood and adolescence through distraction osteogenesis with an external, adjustable, rigid distraction device. *Journal of Craniofacial Surgery*, 8(3):181–185, May 1997.
- [2] J. W. Polley and A. A. Figueroa. Rigid external distraction: Its application in cleft maxillary deformities. *Plastic and Reconstructive Surgery*, 102(5):1360–1372, 1998.
- [3] Th. Hierl and A. Hemprich. A novel modular retention system for midface distraction osteogenesis. *British Journal of Oral and Maxillofacial Surgery*, 38:623–626, 2000.
- [4] F. Watzinger, F. Wanschitz, M. Rasse, W. Millesi, Ch. Schopper, J. Kremser, W. Birkfellner, and R. Ewers. Computer-aided surgery in distraction osteogenesis of the maxilla and mandible. *Int J Oral Maxillofac Surg*, 28(3):171–175, 1999.
- [5] R. S. Nanda. Biomechanical and clinical considerations of a modified protraction headgear. *The American Journal of Orthodontics*, (78):125–139, 1980.
- [6] R. Nanda and W. Hickory. Zygomaticomaxillary suture adaptations incident to anteriorly-directed forces in rhesus monkeys. *Angle Orthod*, 54:199–210, 1984.
- [7] Th. Hierl, R. Klöppel, and A. Hemprich. Midface distraction osteogenesis without major osteotomies: A report on the first clinical application. *Plastic and Reconstruction Surgery*, 108(6):1667–1672, November 2001.
- [8] A. C. Kak and M. Slaney. *Principles of Computerized Tomographic Imaging*. Society of Industrial and Applied Mathematics, Philadelphia (PA), 2001.
- [9] P. Thévenaz, U. E. Ruttimann, and M. Unser. Iterative multi-scale registration without landmarks. In B. Werner, editor, *Proceedings of the 1995 IEEE International Conference on Image Processing (ICIP'95)*, volume III, pages 228–231, Los Alamitos (CA), October 23-26 1995. IEEE Computer Society.
- [10] F. L. Bookstein. Principal warps: Thin-plate splines and the decomposition of deformations. *IEEE Transactions on Pattern Analysis and Machine Intelligence*, 11(6):567–585, 1989.
- [11] W. Beil, K. Rohr, and H. S. Stiel. Investigation of approaches for the localization of anatomical landmarks in 3d medical images. In H. U. Lemke, M. W. Vannier, and K. Inamura, editors, *Proc. Computer Assisted Radiology and Surgery (CAR'97)*, pages 265–270, Amsterdam Lausanne, 1997. Elsevier.
- [12] G. E. Christensen. *Deformable shape models for neuroanatomy*. DSc.-thesis, Server Institut of Technology, Washington University, Saint Louis, 1994.
- [13] W.R. Crum, Griffin L.D., D.L.G. Hill, and D.J. Hawkes. Zen and the art of medical image registration: correspondence, homology, and quality. *Neuroimage*, 20:1425–1437, 2003.
- [14] Michael Meissner and Stefan Guthe. Interactive lighting models and pre-integration for volume rendering on pc graphics accelerators. In *Graphics Interface*. Canadian Information Processing Society, 2002.
- [15] P. Ning and J. Bloomenthal. An evaluation of implicit surface tilers. *Computer Graphics*, 13(6):33–41, Nov/Dec 1993.
- [16] H.H. Hoppe, T. DeRose, T. Duchamp, J.A. McDonald, and W. Stuetzle. Mesh optimization. In J. T. Kajiya, editor, *SIGGRAPH '93 Proceedings*, volume 27 of *Computer Graphics*, pages 19–26, Anaheim (CA), 1993.
- [17] P. Lindstrom and G. Turk. Evaluation of memory-less simplification. *IEEE Transactions on Visualization and Computer Graphics*, 5(2):98–115, 1999.
- [18] R. S. Nanda. Protraction of maxilla in rhesus monkeys by controlled extraoral forces. *Am J Orthod*, (74):121–141, 1978.